Advances in Applied Mathematics and Mechanics
Adv. Appl. Math. Mech., Vol. **10**, No. 6, pp. 1344-1364

DOI: 10.4208/aamm.OA-2017-0241
December 2018

Nonlinear Free Vibration of Reinforced Skew Plates with SWCNs Due to Finite Strain

S. Jafari Mehrabadi[1,*] and S. M. Nodeh Farahani[2]

[1] *Department of Mechanical Engineering, Arak Branch, Islamic Azad University, Arak, Iran*
[2] *Department of Mechanical Engineering, Kashan University, Kashan, Iran*

Received 26 September 2017; Accepted (in revised version) 3 May 2018

Abstract. This paper is an attempt to investigate the nonlinear free vibration of skew plates reinforced by carbon nanotubes (CNTs) due to finite strain tensor. The material properties of the nano-composite are estimated using the molecular dynamic results and the rule of mixture. Also, the differential equations governing the motions are derived on the basis of Classical Plate Theory (CPT) regarding the nonlinear Green-Lagrange strain tensor. In order to solve the nonlinear equations, Galerkin's method, Frechet derivative and differential quadrature method are used. The effects of volume fraction of functionally graded materials (FGM), skew angle, distribution of CNTs and geometrical features of the plate on the nonlinear vibration of system have been studied. The results of this study have been compared with other researches and a good agreement has been achieved.

AMS subject classifications: 34A34

Key words: Finite strains, nonlinear vibration, skew plate, carbon nanotubes, functionally graded materials.

1 Introduction

Skew plates are important structural components in many kinds of high performance surface and aircraft industry for example, they are used in the construction of wings, tails, and fins of swept-wing aircrafts, missiles and skew bridges. There is a large number of papers which focus on the free vibration of thin and thick skew plates. In the following section, some of the relevant studies will be discussed.

Singha and Daripa [1] studied the nonlinear vibration of laminated composite skew plates by finite element method. They used von-Karman's kinematic relations in order to formulate the problem. By applying the Galerkin's method and Newmark's technique,

*Corresponding author.
Email: s-Jafari@iau-arak.ac.ir (S. J. Mehrabadi)

the nonlinear frequency ratio has been investigated with respect to the fiber orientation, skew angle and boundary condition. They found that nonlinear frequency ratio increases by increasing the skew angle and thickness of plate.

Malekzadeh [2] investigated the nonlinear free vibration of thin composite skew plates. In order to derive the governing differential equations, he has used von-Karman's kinematics relations. Obtained equations were solved by generalized differential quadrature (GDQ) method. Finally, nonlinear frequency ratios of plate by considering the skew angle, ratio of thickness-to-width, and amplitude ratios, in different tables have been investigated. Upadhyay and Shukla [3] studied the static and dynamic analysis of functionally graded skew plates under dynamic and static loading. as many published papers, they used nonlinear von-Karman's kinematic relations and Hamilton's principal for obtaining the equations of motions. After solving the governing equations, the effect of skew angle and different boundary conditions on the plate deflection and bending moment have been discussed. Malekzadeh [4] investigated the nonlinear free vibration of thin to moderately laminated skew plates based on the FSDT and DQ method. He used direct iteration technique and harmonic balance method for solving the nonlinear governing equations of motions. At the end, nonlinear frequency ratio in terms of geometrical variables and orientation of fibers have been shown in different figures. Obtained results indicate that DQ method is a powerful technique in solving nonlinear problems. Recently Liew et al. [5] analysed the nonlinear behavior of reinforced laminated composite plates by CNTs. For reinforcing the mentioned plates they applied several distributions of CNTs such as UD, FG-V, FG-O and FG-X type. It is obvious from the results presented in this paper that the non-dimensional central deflections of laminated functionally graded carbon nanotube reinforced (FG- CNTR) plates have been decreased by increasing the volume fraction of carbon nanotubes, since the stiffness of CNTRC plate increases when the volume fraction of carbon nanotubes increases.

Asadi et al. [6] investigated the application of piezoelectric materials and CNTs in nonlinear vibration behaviors of FG-CNTs reinforced composite plates. After solving the governing differential equations by GDQ method the effects of many parameters such as volume fractions of CNTs, thickness of piezoelectric layers and electrical boundary conditions on the nonlinear natural frequencies of system have been discussed. Malekzadeh [7] studied the free vibration of quadrilateral laminated plates with carbon nanotube reinforced composite layers. Distributions of CNTs which are selected include UD, FG-X, FG-V, FG-O and GDQ method used for solving the governing differential equations. Finally, the first three natural frequencies of system in SSSS and CCCC boundary conditions have been determined in a numerical example. Liew et al. [8] derived vibration frequencies and mode shapes of carbon nanotube-reinforced composite skew plates. They used IMLS approximation and Ritz method for solving the problem. At the end of mentioned paper they obtained mode shapes and natural frequencies of plate in terms of thickness-to width ratio and skew angle in different kinds of CNTs distributions. Malekzadeh [9] worked on the low velocity impact of FG-CNT composite skew plates. In this research, deflection of plate under the impact force formulated based on the FSDT and finite element method. Eventually, central deflection of plate in terms of time in two different sets of boundary conditions and different kind of CNTs distributions have been obtained. Following this research, Kiani [10] published a paper about the linear free vibration of FG-CNT reinforced composite skew plates. He applied the Gram-Schmidt's process with suitable shape functions and Ritz method for obtaining the natural frequencies of structure. After that, the first six natural frequencies of plate in different type of CNTs distributions have been determined. Zhang and Xiao [11] calculated the action of a SWCNT-reinforced (Mori-Tanaka approach) laminated composite skew plates subjected to impact loading. The solution of the problem has been done by the element-free IMLS-Ritz method. Finally, mechanical behavior of plate under the effects of skew angle, geometrical features and CNTs orientations have been discussed. To the best of our knowledge no nonlinear free vibration solution has been published on FG-CNTRC skew plates so far.

The present work focuses on the nonlinear free vibration behaviors of skew plate reinforced with single wall carbon nanotubes (SWCNTs) due to finite strains tensor. The effective material properties of nano-composite plates are estimated by the extended rule of mixture. Using Hamilton's principle the governing equations are derived based on the classical plate theory by regarding the nonlinear Green-Lagrange strain tensor. The Galerkin's procedure and Frechet derivative technique and differential quadrature method are employed to solve the nonlinear equations. Because no known results are available for the nonlinear free vibration of functionally graded carbon nanotube-reinforced composite (FG-CNTRC) skew plates, we have to simplify the problem to an isotropic case so that the comparison studies can be carried out. A detailed parametric study is carried out to investigate the influences of CNTs volume fractions, distribution of CNTs, skew angle and geometrical parameters on the nonlinear behaviors of nano-composite skew plate.

2 Modeling properties in skew plate

Consider a CNTRC skew plate with length a, width b, thickness h and skew angle θ shown in Fig. 1.

UD-CNTRC represents the uniform distribution and FG-V, FG-O and FG-X CNTRC are the functionally graded distributions of carbon nanotubes in the thickness direction of the skew plates. The effective material properties of nano-composite skew plate can be estimated according to the Mori-Tanaka scheme or the rule of mixtures approach. Based on the aforementioned rule, it can be written as below:

$$E_{11}=\eta_1 V_{cn}E_{11}^{cn}+V_m E^m, \tag{2.1a}$$

$$\frac{\eta_2}{E_{22}}=\frac{V_{cn}}{E_{22}^{cn}}+\frac{V_m}{E^m}, \tag{2.1b}$$

$$\frac{\eta_3}{G_{12}}=\frac{V_{cn}}{G_{12}^{cn}}+\frac{V_m}{G^m}. \tag{2.1c}$$

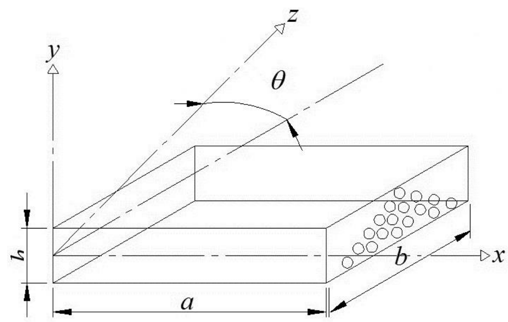

Figure 1: Schematic of reinforced skew plate with coordinates axis (FGA CNTRC).

Where E_{11}^{cn}, E_{22}^{cn} and G_{12}^{cn} are the Young's modulus and shear modulus of the SWCNTs, respectively. Moreover, E^m and G^m are the corresponding properties of the polymer matrix.

η_1, η_2 and η_3 are carbon nanotube efficiency parameter and can be determined by matching the rule of mixture results and molecular dynamic simulation. Also, V_m and V_{cn} are matrix and carbon nanotube volume fractions and are related by the following equation.

$$V_{cn}+V_m=1. \tag{2.2}$$

In above equation, volume fraction and mass ratio of nanotubes are related as below

$$V_{cn}=w(z)\,V_{cn}{}^*. \tag{2.3}$$

In above relation, $w(z)$ is related to the carbon nanotube distribution in thickness direction of plate. The different types of $w(z)$ are introduced as follows:

$$\begin{aligned} &w(z)=1\rightarrow UD,\\ &w(z)=1+2\frac{z}{h}\rightarrow FGV,\\ &w(z)=4\left|\frac{z}{h}\right|\rightarrow FGX,\\ &w(z)=2\left(1-2\left|\frac{z}{h}\right|\right)\rightarrow FGO, \end{aligned} \qquad -\frac{h}{2}\leq z\leq\frac{h}{2}. \tag{2.4}$$

Distribution of carbon nano-tubes in the thickness direction of plate based on the Eq. (2.4) is shown in Fig. 2.

After selecting the distribution models of nanotubes, the Possion's ratio of nanocomposite plate is calculated as below

$$\nu_{12}=V_{cn}\nu_{12}^{cn}+V_m\nu^m. \tag{2.5}$$

In this paper, the PMMA matrix and the single walled carbon nanotubes (10,10) are selected. Material properties of main plate and carbon nano-tubes are listed in Table 1.

Efficiency parameters of carbon nanotubes calculated by molecular dynamic simulation are listed in Table 2.

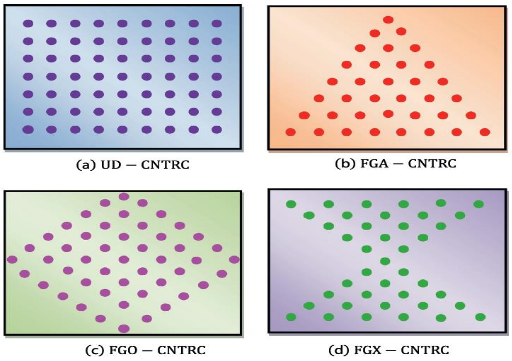

Figure 2: Different combinations of carbon nanotubes in thickness direction of plate.

3 Governing equations

According to Fig. 1, it is assumed that a skew plate with the dimension of $a*b*h$, has been reinforced by the single walled carbon nanotubes (for example type FGA or FGV). The main problem is to calculate the linear and non-linear frequencies of plate vibration under finite strain. In this regard, to achieve the equations of motion, the displacement field is selected based on classical plate theory and may be written as follows:

$$u_1(x,y,z,t)=u(x,y,t)-z\frac{\partial w(x,y,t)}{\partial x}, \tag{3.1a}$$

$$u_2(x,y,z,t)=v(x,y,t)-z\frac{\partial w(x,y,t)}{\partial y}, \tag{3.1b}$$

$$u_3(x,y,z,t)=w(x,y,t). \tag{3.1c}$$

Where u_1, u_2, u_3 are displacement components in x-y-z directions, respectively and u-v-w are displacement components of neutral surface of plate.

In the next step, according to the Green's-Lagrange's strain-displacement tensor, the components of displacement tensor are calculated as follows

$$E_{ij}=\frac{1}{2}\left(u_{i,j}+u_{j,i}+u_{m,i}u_{m,j}\right). \tag{3.2}$$

By substituting the Eq. (3.1) into the Eq. (3.2), the components of strain tensor can be written as

$$\varepsilon_1=\varepsilon_x=\varepsilon_x^0+z\varepsilon_x^1+z^2\varepsilon_x^2, \tag{3.3a}$$

$$\varepsilon_2=\varepsilon_y=\varepsilon_y^0+z\varepsilon_y^1+z^2\varepsilon_y^2, \tag{3.3b}$$

$$\varepsilon_6=\gamma_{xy}=\gamma_{xy}^0+z\gamma_{xy}^1+z^2\gamma_{xy}^2. \tag{3.3c}$$

Where the terms of aforesaid equations are

$$\begin{cases} \varepsilon_x^0 = \dfrac{\partial u}{\partial x} + \dfrac{1}{2}\left(\dfrac{\partial u}{\partial x}\right)^2 + \dfrac{1}{2}\left(\dfrac{\partial v}{\partial x}\right)^2 + \dfrac{1}{2}\left(\dfrac{\partial w}{\partial x}\right)^2, \\ \varepsilon_x^1 = -\dfrac{\partial^2 w}{\partial x^2} - \dfrac{\partial u}{\partial x}\dfrac{\partial^2 w}{\partial x^2} - \dfrac{\partial v}{\partial x}\dfrac{\partial^2 w}{\partial x \partial y}, \\ \varepsilon_x^2 = \dfrac{1}{2}\left(\dfrac{\partial^2 w}{\partial x^2}\right)^2 + \dfrac{1}{2}\left(\dfrac{\partial^2 w}{\partial x \partial y}\right)^2, \end{cases} \tag{3.4a}$$

$$\begin{cases} \varepsilon_y^0 = \dfrac{\partial v}{\partial y} + \dfrac{1}{2}\left(\dfrac{\partial u}{\partial y}\right)^2 + \dfrac{1}{2}\left(\dfrac{\partial v}{\partial y}\right)^2 + \dfrac{1}{2}\left(\dfrac{\partial w}{\partial y}\right)^2, \\ \varepsilon_y^1 = -\dfrac{\partial^2 w}{\partial y^2} - \dfrac{\partial v}{\partial y}\dfrac{\partial^2 w}{\partial y^2} - \dfrac{\partial u}{\partial y}\dfrac{\partial^2 w}{\partial x \partial y}, \\ \varepsilon_y^2 = \dfrac{1}{2}\left(\dfrac{\partial^2 w}{\partial y^2}\right)^2 + \dfrac{1}{2}\left(\dfrac{\partial^2 w}{\partial x \partial y}\right)^2, \end{cases} \tag{3.4b}$$

$$\begin{cases} \gamma_{xy}^0 = \dfrac{\partial u}{\partial y} + \dfrac{\partial v}{\partial x} + \dfrac{\partial u}{\partial x}\dfrac{\partial u}{\partial y} + \dfrac{\partial v}{\partial x}\dfrac{\partial v}{\partial y} + \dfrac{\partial w}{\partial x}\dfrac{\partial w}{\partial y}, \\ \gamma_{xy}^1 = -2\dfrac{\partial^2 w}{\partial x \partial y} - \dfrac{\partial u}{\partial x}\dfrac{\partial^2 w}{\partial x \partial y} - \dfrac{\partial u}{\partial y}\dfrac{\partial^2 w}{\partial x^2} - \dfrac{\partial v}{\partial x}\dfrac{\partial^2 w}{\partial y^2} - \dfrac{\partial v}{\partial y}\dfrac{\partial^2 w}{\partial x \partial y}, \\ \gamma_{xy}^2 = \dfrac{\partial^2 w}{\partial x^2}\dfrac{\partial^2 w}{\partial x \partial y} + \dfrac{\partial^2 w}{\partial y^2}\dfrac{\partial^2 w}{\partial x \partial y}. \end{cases} \tag{3.4c}$$

Note that other components of strain tensor are zero.

For calculating the strain energy of system, we assume that the plate would be under the state of plain stress. The stress-strain relationships will be written as below:

$$\begin{Bmatrix} \sigma_1 \\ \sigma_2 \\ \sigma_6 \end{Bmatrix} = \begin{Bmatrix} \sigma_x \\ \sigma_y \\ \tau_{xy} \end{Bmatrix} = \begin{bmatrix} Q_{11} & Q_{12} & 0 \\ Q_{21} & Q_{22} & 0 \\ 0 & 0 & Q_{66} \end{bmatrix} \begin{Bmatrix} \varepsilon_1 \\ \varepsilon_2 \\ \varepsilon_6 \end{Bmatrix}. \tag{3.5}$$

Where the coefficients of stiffness matrix are given by:

$$Q_{11} = \frac{E_{11}}{1-\nu_{12}\nu_{21}}, \qquad Q_{12} = \frac{\nu_{12}E_{22}}{1-\nu_{12}\nu_{21}}, \tag{3.6a}$$

$$Q_{21} = \frac{\nu_{21}E_{11}}{1-\nu_{12}\nu_{21}}, \qquad Q_{22} = \frac{E_{22}}{1-\nu_{12}\nu_{21}}, \tag{3.6b}$$

$$Q_{66} = G_{12}. \tag{3.6c}$$

In the aforementioned relationships, the quantities of E_{11}, E_{22}, G_{12}, ν_{12}, $\nu_{21}$are the effective properties of material and can be calculated using the Mori-Tanaka scheme and the rule of mixtures approach.

By substituting the Eqs. (3.4) in (3.5), the components of plate stress in terms of non-linear strain will be as follows:

$$\sigma_x=Q_{11}\varepsilon_x+Q_{11}\varepsilon_y=Q_{11}\left[\varepsilon_x^0+z\varepsilon_x^1+z^2\varepsilon_x^2\right]+Q_{12}\left[\varepsilon_y^0+z\varepsilon_y^1+z^2\varepsilon_y^2\right], \tag{3.7a}$$

$$\sigma_y=Q_{12}\varepsilon_x+Q_{22}\varepsilon_y=Q_{12}\left[\varepsilon_x^0+z\varepsilon_x^1+z^2\varepsilon_x^2\right]+Q_{22}\left[\varepsilon_y^0+z\varepsilon_y^1+z^2\varepsilon_y^2\right], \tag{3.7b}$$

$$\tau_{xy}=Q_{66}\gamma_{xy}=Q_{66}\left[\gamma_{xy}^0+z\gamma_{xy}^1+z^2\gamma_{xy}^2\right], \tag{3.7c}$$

For the simplicity of results, the resultant forces and moments of plate can be defined as below

$$N_i=\int_{-\frac{h}{2}}^{\frac{h}{2}}\sigma_i dz,\quad M_i=\int_{-\frac{h}{2}}^{\frac{h}{2}}z\sigma_i dz,\quad P_i=\int_{-\frac{h}{2}}^{\frac{h}{2}}z^2\sigma_i dz,\qquad i=1,2,6. \tag{3.8}$$

Also, we introduce stiffness matrices as follows:

$$[A]_{ij}=\int_{-\frac{h}{2}}^{\frac{h}{2}}[Q]_{ij}dz,\qquad [B]_{ij}=\int_{-\frac{h}{2}}^{\frac{h}{2}}[Q]_{ij}zdz,\qquad [D]_{ij}=\int_{-\frac{h}{2}}^{\frac{h}{2}}[Q]_{ij}z^2dz, \tag{3.9a}$$

$$[F]_{ij}=\int_{-\frac{h}{2}}^{\frac{h}{2}}[Q]_{ij}z^3dz,\qquad [H]_{ij}=\int_{-\frac{h}{2}}^{\frac{h}{2}}[Q]_{ij}z^4dz. \tag{3.9b}$$

Where $[A]_{ij}$ is the extensional stiffness matrix, $[B]_{ij}$ is the bending-extensional coupling stiffness matrix, and $[D]_{ij}$ is the bending stiffness matrix. $[F]_{ij}$ and $[H]_{ij}$ are higher order stiffness matrices.

By the above-mentioned matrices, the resultant stresses of M, N, and P can be rewritten as below

$$\begin{aligned}N_i&=\int_{-\frac{h}{2}}^{\frac{h}{2}}\sigma_i dz=\int_{-\frac{h}{2}}^{\frac{h}{2}}[Q]_{ij}\varepsilon_j dz=\int_{-\frac{h}{2}}^{\frac{h}{2}}[Q]_{ij}\left[\varepsilon_j^0+z\varepsilon_j^1+z^2\varepsilon_j^2\right]dz\\&=[A]_{ij}\left\{\varepsilon_j^0\right\}+[B]_{ij}\left\{\varepsilon_j^1\right\}+[D]_{ij}\left\{\varepsilon_j^2\right\},\end{aligned} \tag{3.10a}$$

$$\begin{aligned}M_i&=\int_{-\frac{h}{2}}^{\frac{h}{2}}\sigma_i zdz=\int_{-\frac{h}{2}}^{\frac{h}{2}}[Q]_{ij}\varepsilon_j zdz=\int_{-\frac{h}{2}}^{\frac{h}{2}}[Q]_{ij}\left[\varepsilon_j^0+z\varepsilon_j^1+z^2\varepsilon_j^2\right]zdz\\&=[B]_{ij}\left\{\varepsilon_j^0\right\}+[D]_{ij}\left\{\varepsilon_j^1\right\}+[F]_{ij}\left\{\varepsilon_j^2\right\},\end{aligned} \tag{3.10b}$$

$$\begin{aligned}P_i&=\int_{-\frac{h}{2}}^{\frac{h}{2}}\sigma_i z^2dz=\int_{-\frac{h}{2}}^{\frac{h}{2}}[Q]_{ij}\varepsilon_j z^2dz=\int_{-\frac{h}{2}}^{\frac{h}{2}}[Q]_{ij}\left[\varepsilon_j^0+z\varepsilon_j^1+z^2\varepsilon_j^2\right]z^2dz\\&=[D]_{ij}\left\{\varepsilon_j^0\right\}+[F]_{ij}\left\{\varepsilon_j^1\right\}+[H]_{ij}\left\{\varepsilon_j^2\right\}.\end{aligned} \tag{3.10c}$$

Since the Hamilton's principle is to be used, the variation of potential energy of system is first calculated by the below equation

$$U=\frac{1}{2}\int_v(\sigma_{ij}\varepsilon_{ij})dV\Rightarrow\delta U=\int_v(\sigma_{ij}\delta\varepsilon_{ij})dV=\int_v\left(\sigma_x\delta\varepsilon_x+\sigma_y\delta\varepsilon_y+\sigma_{xy}\delta\gamma_{xy}\right)dV. \tag{3.11}$$

By substituting Eq. (3.10) in the aforementioned equation, it yields

$$\delta U=\int_A\left\{\begin{array}{c} N_x\delta\varepsilon_x^0+M_x\delta\varepsilon_x^1+P_x\delta\varepsilon_x^2+N_y\delta\varepsilon_y^0+M_y\delta\varepsilon_y^1 \\ +P_y\delta\varepsilon_y^2+N_{xy}\delta\gamma_{xy}^0+M_{xy}\delta\gamma_{xy}^1+P_{xy}\delta\gamma_{xy}^2 \end{array}\right\}dA. \tag{3.12}$$

Also the kinetic energy of plate can be written as follows

$$\begin{aligned}\delta T&=\int_v\rho(\dot{u}_1\delta\dot{u}_1+\dot{u}_2\delta\dot{u}_2+\dot{u}_3\delta\dot{u}_3)dV\\ &=\int_v\rho\left\{\left(\dot{u}-z\frac{\partial\dot{w}}{\partial x}\right)\left(\delta\dot{u}-z\frac{\partial\delta\dot{w}}{\partial x}\right)+\left(\dot{v}-z\frac{\partial\dot{w}}{\partial y}\right)\left(\delta\dot{v}-z\frac{\partial\delta\dot{w}}{\partial y}\right)+\dot{w}\delta\dot{w}\right\}dV.\end{aligned} \tag{3.13}$$

Terms of inertia moments of plates are defined in the following form

$$(I_0,I_1,I_2)=\int_{-\frac{h}{2}}^{\frac{h}{2}}\rho(1,z,z^2)dz. \tag{3.14}$$

By substituting the Eq. (3.14) into Eq. (3.13) the following relation is obtained

$$\delta T=\int_A\left\{\begin{array}{l} I_0\dot{u}\delta\dot{u}-I_1\dot{u}\dfrac{\partial\delta\dot{w}}{\partial x}-I_1\dfrac{\partial\dot{w}}{\partial x}\delta\dot{u}+I_2\dfrac{\partial\dot{w}}{\partial x}\dfrac{\partial\delta\dot{w}}{\partial x} \\ +I_0\dot{v}\delta\dot{v}-I_1\dot{v}\dfrac{\partial\delta\dot{w}}{\partial y}-I_1\dfrac{\partial\dot{w}}{\partial y}\delta\dot{v}+I_2\dfrac{\partial\dot{w}}{\partial y}\dfrac{\partial\delta\dot{w}}{\partial y}+I_0\dot{w}\delta\dot{w} \end{array}\right\}dA. \tag{3.15}$$

Using Hamilton's principal, the following equation will be obtained

$$\begin{aligned}&\frac{\partial N_x}{\partial x}+\frac{\partial N_{xy}}{\partial y}+\frac{\partial}{\partial x}\left(N_x\frac{\partial u}{\partial x}\right)+\frac{\partial}{\partial x}\left(N_{xy}\frac{\partial u}{\partial y}\right)+\frac{\partial}{\partial y}\left(N_{xy}\frac{\partial u}{\partial x}\right)+\frac{\partial}{\partial y}\left(N_y\frac{\partial u}{\partial y}\right)\\ &-\frac{\partial}{\partial x}\left(M_x\frac{\partial^2 w}{\partial x^2}\right)-\frac{\partial}{\partial x}\left(M_{xy}\frac{\partial^2 w}{\partial x\partial y}\right)-\frac{\partial}{\partial y}\left(M_{xy}\frac{\partial^2 w}{\partial x^2}\right)-\frac{\partial}{\partial y}\left(M_y\frac{\partial^2 w}{\partial x\partial y}\right)\\ &=I_0\frac{\partial^2 u}{\partial t^2}-I_1\frac{\partial^3 w}{\partial x\partial t^2},\end{aligned} \tag{3.16a}$$

$$\begin{aligned}&\frac{\partial N_y}{\partial y}+\frac{\partial N_{xy}}{\partial x}+\frac{\partial}{\partial x}\left(N_x\frac{\partial v}{\partial x}\right)+\frac{\partial}{\partial x}\left(N_{xy}\frac{\partial v}{\partial y}\right)+\frac{\partial}{\partial y}\left(N_{xy}\frac{\partial v}{\partial x}\right)+\frac{\partial}{\partial y}\left(N_y\frac{\partial v}{\partial y}\right)\\ &-\frac{\partial}{\partial x}\left(M_x\frac{\partial^2 w}{\partial x\partial y}\right)-\frac{\partial}{\partial x}\left(M_{xy}\frac{\partial^2 w}{\partial y^2}\right)-\frac{\partial}{\partial y}\left(M_{xy}\frac{\partial^2 w}{\partial x\partial y}\right)-\frac{\partial}{\partial y}\left(M_y\frac{\partial^2 w}{\partial y^2}\right)\\ &=I_0\frac{\partial^2 v}{\partial t^2}-I_1\frac{\partial^3 w}{\partial y\partial t^2},\end{aligned} \tag{3.16b}$$

$$\begin{aligned}&\frac{\partial^2 M_x}{\partial x^2}+2\frac{\partial^2 M_{xy}}{\partial x\partial y}+\frac{\partial^2 M_y}{\partial y^2}+\frac{\partial}{\partial x}\left(N_x\frac{\partial w}{\partial x}\right)+\frac{\partial}{\partial x}\left(N_{xy}\frac{\partial w}{\partial y}\right)+\frac{\partial}{\partial y}\left(N_{xy}\frac{\partial w}{\partial x}\right)+\frac{\partial}{\partial y}\left(N_y\frac{\partial w}{\partial y}\right)\\ &+\frac{\partial^2}{\partial x^2}\left(M_x\frac{\partial u}{\partial x}\right)+\frac{\partial^2}{\partial x\partial y}\left(M_x\frac{\partial v}{\partial x}\right)+\frac{\partial^2}{\partial x^2}\left(M_{xy}\frac{\partial u}{\partial y}\right)+\frac{\partial^2}{\partial x\partial y}\left(M_{xy}\frac{\partial u}{\partial x}\right)+\frac{\partial^2}{\partial x\partial y}\left(M_{xy}\frac{\partial v}{\partial y}\right)\end{aligned}$$

$$
\begin{aligned}
&+\frac{\partial^2}{\partial y^2}\left(M_{xy}\frac{\partial v}{\partial x}\right)+\frac{\partial^2}{\partial x\partial y}\left(M_y\frac{\partial u}{\partial y}\right)+\frac{\partial^2}{\partial y^2}\left(M_y\frac{\partial v}{\partial y}\right)-\frac{\partial^2}{\partial x^2}\left(P_x\frac{\partial^2 w}{\partial x^2}\right)-\frac{\partial^2}{\partial x\partial y}\left(P_x\frac{\partial^2 w}{\partial x\partial y}\right)\\
&-\frac{\partial^2}{\partial x^2}\left(P_{xy}\frac{\partial^2 w}{\partial x\partial y}\right)-\frac{\partial^2}{\partial x\partial y}\left(P_{xy}\frac{\partial^2 w}{\partial x^2}\right)-\frac{\partial^2}{\partial x\partial y}\left(P_{xy}\frac{\partial^2 w}{\partial y^2}\right)-\frac{\partial^2}{\partial y^2}\left(P_{xy}\frac{\partial^2 w}{\partial x\partial y}\right)\\
&-\frac{\partial^2}{\partial x\partial y}\left(P_y\frac{\partial^2 w}{\partial x\partial y}\right)-\frac{\partial^2}{\partial y^2}\left(P_y\frac{\partial^2 w}{\partial y^2}\right)\\
&=I_0\frac{\partial^2 w}{\partial t^2}+I_1\frac{\partial^3 u}{\partial x\partial t^2}+I_1\frac{\partial^3 v}{\partial y\partial t^2}-I_2\frac{\partial^4 w}{\partial x^2\partial t^2}-I_2\frac{\partial^4 w}{\partial y^2\partial t^2}. \qquad (3.16c)
\end{aligned}
$$

In order to solve the mentioned equations, we should write those equations in terms of displacement. For this reason, the resultant forces and moments are first written in terms of strain components and then, those obtained equations are converted in terms of displacement components (see Appendix).

Because of the prolongation of motion equations, they have not been written here. It should be mentioned that the boundary conditions of plate should be written in terms of displacement components for solving the equations.

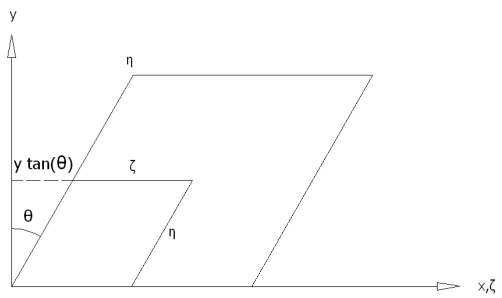

Figure 3: Converting the rectangular coordinate to the parallelogram one.

Afterwards, to achieve the equations of motion for skew plate regarding (Fig. 3), the transformation relationship of rectangular coordinate to the parallelogram one is presented using the relation (3.17)

$$x=\zeta+\eta\sin(\theta), \quad y=\eta\cos(\theta). \qquad (3.17)$$

Using the partial differential rule in new coordinate, we will have the following equation

$$\left\{\begin{array}{c}\dfrac{\partial}{\partial x}\\ \dfrac{\partial}{\partial y}\end{array}\right\}=\begin{bmatrix}1 & 0\\ -\tan\theta & \sec\theta\end{bmatrix}\left\{\begin{array}{c}\dfrac{\partial}{\partial \varsigma}\\ \dfrac{\partial}{\partial \eta}\end{array}\right\}, \qquad (3.18a)$$

$$\left\{\begin{array}{c}\frac{\partial^2}{\partial x^2}\\ \frac{\partial^2}{\partial x\partial y}\\ \frac{\partial^2}{\partial y^2}\end{array}\right\}=\begin{bmatrix}1 & 0 & 0\\ -\tan\theta & \sec\theta & 0\\ \tan^2\theta & -2\sec\theta\tan\theta & \sec^2\theta\end{bmatrix}\left\{\begin{array}{c}\frac{\partial^2}{\partial \varsigma^2}\\ \frac{\partial^2}{\partial \varsigma\partial\eta}\\ \frac{\partial^2}{\partial \eta^2}\end{array}\right\}, \tag{3.18b}$$

$$\left\{\begin{array}{c}\frac{\partial^4}{\partial x^4}\\ \frac{\partial^4}{\partial x^2\partial y^2}\\ \frac{\partial^4}{\partial y^4}\end{array}\right\}=\begin{bmatrix}1 & 0 & 0 & 0 & 0\\ \tan^2\theta & -2\sec\theta\tan\theta & \sec^2\theta & 0 & 0\\ -\tan^4\theta & -4\sec\theta\tan^3\theta & 6\sec^2\theta\tan^2\theta & -4\sec^3\theta\tan\theta & \sec^4\theta\end{bmatrix}$$

$$\cdot\left\{\begin{array}{c}\frac{\partial^4}{\partial \varsigma^4}\\ \frac{\partial^4}{\partial \varsigma^3\partial\eta}\\ \frac{\partial^4}{\partial \varsigma^2\partial\eta^2}\\ \frac{\partial^4}{\partial \varsigma\partial\eta^3}\\ \frac{\partial^4}{\partial \eta^4}\end{array}\right\}. \tag{3.18c}$$

By applying the Eqs. (3.18a) and (3.18c) to those of motion equations and boundary conditions of skew plate, the governing equations and boundary conditions of system in new coordinate (ζ,η) will be derived. Note that for simplicity, ζ and η were substituted by x and y, respectively. Now, the following answers of u, v and w are considered for solving the mentioned equations

$$u(x,y,t)=U(x,y)\cos(\omega t), \tag{3.19a}$$

$$v(x,y,t)=V(x,y)\cos(\omega t), \tag{3.19b}$$

$$w(x,y,t)=W(x,y)\cos(\omega t). \tag{3.19c}$$

Where ω is the natural frequency of plate vibration. Next, the residual of each equation can be calculated by applying Galerkin's technique and the system of non-linear algebraic equations is obtained. Because the analytical solution of aforesaid equations is impossible, they should be linearized. For this purpose, the Frechet derivative is used and the mentioned equations are converted with respect to the auxiliary variables of α_1, α_2, α_3, [16]. Afterwards, the equations of motion will be converted to the system of linear algebraic equations and will be solved by simple techniques. For the clarification of solution steps, the operator form of equations will be written and the procedure can be explained as follows

$$\begin{array}{ll} L_1(U,V,W)=0, & \\ L_2(U,V,W)=0, & 0\le x\le a, \\ L_3(U,V,W)=0, & 0\le y\le b. \end{array} \tag{3.20}$$

Where L_1, L_2, L_3 are nonlinear differential operators. These equations can be converted to Eq. (3.21) using the auxiliary variables of α_1, α_2, α_3,

$$L_1'(\alpha_1,\alpha_2,\alpha_3)+L_1(U,V,W)=0, \tag{3.21a}$$

$$L_2'(\alpha_1,\alpha_2,\alpha_3)+L_2(U,V,W)=0, \tag{3.21b}$$

$$L_2'(\alpha_1,\alpha_2,\alpha_3)+L_2(U,V,W)=0. \tag{3.21c}$$

In the written equations, $L'_i(\alpha_1,\ \alpha_2,\ \alpha_3)$, $i=1,\cdots,3$ are the Frechet derivatives that are linear with regard to α_1, α_2, α_3, and nonlinear in terms of u, v and w [16]

$$L'_i(\alpha_1,\alpha_2,\alpha_3)=\frac{\partial(L_i(U+\varepsilon\alpha_1,V+\varepsilon\alpha_2,W+\varepsilon\alpha_3))}{\partial\varepsilon}\bigg|_{\varepsilon=0}, \quad i=1,\cdots,3. \tag{3.22}$$

In order to complete the solution steps, the following repeat-correction process is assumed

$$U^{(n+1)}=U^{(n)}+\alpha_1{}^{(n)}, \tag{3.23a}$$

$$V^{(n+1)}=V^{(n)}+\alpha_2{}^{(n)}, \tag{3.23b}$$

$$W^{(n+1)}=W^{(n)}+\alpha_3{}^{(n)}. \tag{3.23c}$$

In the above equation (3.23), n is the iteration count.

Generally the solving method is in a way that at first the initial guess is considered for U, V and W and then the linear equations (3.21) are solved using GDQ method and α_1, α_2, α_3 are obtained. Then using obtained α_1, α_2, α_3, the Eqs. (3.23) are corrected and the new values of U, V and W are calculated. This cycle is continued to satisfy convergence criterion. The convergence criterion is in the following form

$$\frac{\left\|S^{(n+1)}\right\|}{\left\|S^{(n)}\right\|}\le\varepsilon, \quad \|S\|=\sqrt{\sum_{i=1}^{n}(\alpha_{1i}^2+\alpha_{2i}^2+\alpha_{3i}^2)}. \tag{3.24}$$

In the above relation ε is the small convergence tolerance.

4 Results and discussion

To validate the presented approach and demonstrate its usefulness, convergence studies are carried out, and the results are compared with similar papers in other literatures.

Table 1: Material properties of plate and carbon nanotubes.

$E_{11}^{cnt}=5646.6\text{GPa}$	$E^m=2.5\text{GPa}$
$E_{22}^{cnt}=7080\text{GPa}$	$\nu_m=0.34\text{GPa}$
$G_{12}^{cnt}=1944.5\text{GPa}$	$\rho^m=1150\text{Kg/m}^3$
$\nu_{12}^{cnt}=0.175$	
$\rho^{cnt}=100\text{Kg/m}^3$	

Table 2: Efficiency parameters of carbon nanotubes in different values of volume fraction.

Efficiency parameters	V_{cnt}		
	0.12	0.17	0.28
η_1	0.141	0.142	0.137
η_2	1.585	1.626	1.022
η_3	1.109	1.138	0.715

Table 3: Non-dimensional natural frequency of reinforced skew plate with UD distribution of SWCN-s and CCCC boundary conditions $(h/a=0.001)$.

		$\Omega=\frac{\omega a^2}{\pi^2}\sqrt{\frac{\rho_m h}{D_m}}$								
		$V_{cnt}=0.12$			$V_{cnt}=0.17$			$V_{cnt}=0.28$		
		present	Enrique García et al. (2015)	Zhang et al. (2014)	present	Enrique García et al. (2015)	Zhang et al. (2014)	present	Enrique García et al. (2015)	Zhang et al. (2014)
$\theta=0$	Ω_1	13.054	13.304	13.249	15.792	16.027	15.771	19.745	20.017	19.223
	Ω_2	21.472	21.848	20.951	17.714	18.087	17.761	14.382	14.803	14.715
	Ω_3	26.017	26.734	25.424	22.600	23.327	22.680	17.853	18.686	18.403
	Ω_4	34.652	35.729	33.383	31.432	32.514	31.033	23.172	25.623	24.780
$\theta=30$	Ω_1	20.160	20.550	19.733	16.264	16.625	16.357	13.447	13.741	13.683
	Ω_2	22.934	23.809	22.806	19.278	20.164	19.775	15.672	16.351	16.234
	Ω_3	29.132	31.369	29.738	25.693	27.931	27.077	20.498	22.205	21.802
	Ω_4	39.190	43.849	40.814	35.593	40.080	38.157	28.091	31.566	30.431
$\theta=45$	Ω_1	21.321	21.999	21.120	17.559	18.194	17.895	14.395	14.901	14.833
	Ω_2	26.801	28.389	27.139	23.211	24.770	24.239	18.648	19.853	19.669
	Ω_3	37.565	40.720	38.445	33.674	36.695	35.440	26.713	29.062	28.425
	Ω_4	53.004	57.205	53.565	45.698	47.034	45.846	37.401	38.750	38.183
$\theta=60$	Ω_1	27.144	27.984	26.831	23.390	24.306	23.868	18.708	19.519	19.402
	Ω_2	40.691	42.701	40.628	36.180	38.184	37.166	28.584	30.336	29.903
	Ω_3	60.238	63.394	59.556	53.285	56.232	54.087	41.961	44.851	43.674
	Ω_4	68.432	68.706	65.323	58.026	58.847	57.295	46.437	47.506	46.823

For this object, the governing equations (3.16) are solved in the case of linear free vibration of clamped carbon nanotube reinforced (CNTR) skew plates with mechanical specification inserted in Tables 1 and 2, then the obtained results are compared with similar papers in Table 3.

From the data prepared in the above table, Close agreement between the results of the present approach and other papers is considerable.

Also for validating the present nonlinear solving method, the nonlinear free vibration analysis of isotropic square plate is carried out with simply supported and clamp boundary conditions.

The obtained results are compared with other references in Tables 4 and 5. It is found from obtained results that a good agreement is existed between the results of the present approach.

In the following, the nonlinear free vibration analysis of CNTR skew plate is carried out for different boundary conditions, different distribution of carbon nano tubes and skew angle of plate.

Based on Table 6, it can be said that the maximum nonlinear frequency ratio is related

Table 4: Comparing the aspect ratio of ω_{NI}/ω_L for isotropic square plate with SSSS boundary conditions $(h/a=0.001)$.

References	$W_{\max}/h$				
	0.2	0.4	0.6	0.8	1
Present	1.0145	1.0568	1.1239	1.2116	1.3158
Rao et al. (1976)	1.0149	1.0583	1.1270	1.2166	1.3230
Error (%)	0.039%	0.141%	0.275%	0.412%	0.547%
Mei (1973) and Rao et al. (1993)	1.0134	1.0518	1.1154	1.1946	1.2967
Error (%)	0.108%	0.473%	0.756%	1.403%	1.451%
Singah and Daripa (2007)	1.0080	1.0610	1.1498	1.2641	1.3958
Error(%)	0.640%	0.397%	2.304%	4.333%	6.079%
Shih and Blotter (1993)	1.020	1.076	1.164	1.277	1.410
Error (%)	0.542%	1.816%	3.567%	5.397%	7.159%

Table 5: Comparing the aspect ratio of ω_{NI}/ω_L for isotropic square plate with CCCC boundary conditions $(h/a=0.001)$.

References	$W_{\max}/h$				
	0.2	0.4	0.6	0.8	1
Present	1.0078	1.0310	1.0686	1.1189	1.1806
Rao and Sheikh (1993)	1.0095	1.0375	1.0285	1.1424	1.2149
Error (%)	0.170%	0.630%	1.300%	2.101%	2.905%
Singah and Daripa (2007)	1.0091	1.0297	1.0582	1.0987	1.1537
Error (%)	0.128%	0.126%	0.972%	1.805%	2.278%
Lau et al. (1984)	1.0073	1.0291	1.0648	1.1138	1.1762
Error (%)	0.049	0,184%	0.355%	0.455%	0.372%

to the square plate and decreases with the increased skew angle. Moreover, in all studied plates, the nonlinear frequency ratio increases by increasing the amplitude of vibration, indicating hardening type of nonlinear behavior. Unlike the linear analysis in FGO type of distribution of CNTs, the nonlinear frequency ratio is maximum and UD, FGV and FGX models are put in the next category.

In Table 7, we can see that in case of $V_{cnt}=0.12$, the nonlinear frequency ratio would be maximum and the nonlinear frequency ratio decreases by increasing the CNTs volume fraction. Also, the square plate has the maximum nonlinear frequency ratio and this ratio will be decreased by increasing the skew angle. The behavior, in general, is qualitatively similar to those of simply supported case (Table 6). It can be further concluded that although the type of nonlinear behavior is hardening, the degree of nonlinearity is less compared to those of simply supported skew plates.

Based on Table 8, it can be said that the nonlinear frequency ratio increases as the aspect ratio of $W_{\max}/h$ increases. Regarding all the values of skew angle, the maximum and minimum nonlinear frequency ratio are related to the FGO and FGX type of CNTs distributions, respectively. Note that, specifying the mode shapes in all cases is uncomplicated. By substituting the frequencies of vibration into equations of motion the mode

Table 6: Values of aspect ratio of ω_{NI}/ω_L for reinforced skew plate with SSSS boundary conditions (h/a=0.001 & $a=b$ & $V_{cnt}=0.12$.)

		$W_{\max}/h$				
		0.2	0.4	0.6	0.8	1
$\theta=0$	UD	1.1898	1.6224	2.1677	2.7564	3.3860
	FGV	1.1897	1.6222	2.1674	2.7559	3.3854
	FGO	1.3166	1.9834	2.9670	3.5687	4.3974
	FGX	1.1403	1.5085	1.8456	2.6973	2.9919
$\theta=30$	UD	1.1892	1.6205	2.1645	2.7519	3.3802
	FGV	1.1890	1.6201	2.1639	2.7510	3.3791
	FGO	1.3074	1.9588	2.7172	3.5139	4.3279
	FGX	1.1396	1.5012	1.9602	2.6938	2.9804
$\theta=45$	UD	1.1858	1.6199	2.1574	2.7380	3.3393
	FGV	1.1855	1.6191	2.1560	2.7360	3.3368
	FGO	1.3001	1.9392	2.6854	3.4702	4.2725
	FGX	1.1386	1.4961	1.9538	2.6661	2.9609
$\theta=60$	UD	1.1748	1.5877	2.1027	2.6613	3.2410
	FGV	1.1742	1.5859	2.0997	2.6571	3.2356
	FGO	1.2468	1.7940	2.4478	3.1423	3.8556
	FGX	1.1352	1.4680	1.8970	2.3706	2.8667
$\theta=75$	UD	1.0250	1.0966	1.2065	1.3454	1.5053
	FGV	1.0248	1.0958	1.2048	1.3427	1.5015
	FGO	1.0286	1.1098	1.2334	1.3881	1.5646
	FGX	1.0221	1.0858	1.1843	1.3098	1.4553

shapes can be specified. For example in Fig. 4 the 3D vibration mode shapes of fully clamped UD-CNTRC skew plate ($V_{cnt}=0.12$, $a=b=1$ and $h/a=0.01$) for different skew angles are plotted.

5 Conclusions

In this paper, nonlinear free vibration behaviors of skew plates reinforced with single wall carbon nanotubes (SWCNTs) are presented.

Using Hamilton principle the governing equations are derived based on the classical plate theory by regarding the nonlinear Green-Lagrange strain tensor. The Galerkin procedure and Frechet derivative technique with differential quadrature method are employed to solve the nonlinear equations.

The accuracy of the GDQ method with Frechet derivative technique is demonstrated by convergence and comparison studies. A close agreement is achieved for the comparison studies of these skew and square plates. These comparison studies in nonlinear analysis are possible only for the isotropic plates because no existing results are available for the nonlinear free vibration of FG-CNTRC skew plates.

The influences of carbon nanotube volume fraction, skew angles, and distribution of

Table 7: Aspect ratio of ω_{Nl}/ω_L for reinforced skew plate with UD distribution of CNT-s and CCCC boundary conditions ($h/a=0.001$ & $a=b$).

Skew angle & volume fraction		$W_{\max}/h$				
		0.2	0.4	0.6	0.8	1
$\theta=0$	$V_{cnt}=0.12$	1.0474	1.1781	1.3685	1.5974	1.8505
	$V_{cnt}=0.17$	1.0471	1.1771	1.3666	1.5945	1.8466
	$V_{vnt}=0.28$	1.0468	1.1766	1.3645	1.5913	1.8414
$\theta=30$	$V_{cnt}=0.12$	1.0458	1.1725	1.3576	1.5808	1.8281
	$V_{cnt}=0.17$	1.0452	1.1705	1.3538	1.5749	1.8202
	$V_{vnt}=0.28$	1.0446	1.1693	1.3481	1.5692	1.8117
$\theta=45$	$V_{cnt}=0.12$	1.0448	1.1690	1.3508	1.5703	1.8139
	$V_{cnt}=0.17$	1.0439	1.1657	1.3443	1.5605	1.8006
	$V_{cnt}=0.28$	1.0428	1.1623	1.3376	1.5513	1.7884
$\theta=60$	$V_{cnt}=0.12$	1.0368	1.1402	1.2942	1.4832	1.6955
	$V_{cnt}=0.17$	1.0359	1.1369	1.2877	1.4731	1.6817
	$V_{cnt}=0.28$	1.0338	1.1346	1.2851	1.4701	1.6783
$\theta=75$	$V_{cnt}=0.12$	1.0159	1.0621	1.1350	1.2298	1.3419
	$V_{cnt}=0.17$	1.0158	1.0618	1.1343	1.2287	1.3403
	$V_{cnt}=0.28$	1.0138	1.0597	1.1321	1.2262	1.3376

Table 8: Values of aspect ratio ω_{Nl}/ω_L for reinforced skew plate with SCSC boundary conditions ($h/a=0.001$ & $a=b$).

		$W_{\max}/h$				
		0.2	0.4	0.6	0.8	1
$\theta=0$	UD	1.1529	1.5222	1.9908	2.5037	3.0384
	FGV	1.1521	1.5196	1.9864	2.4974	3.0303
	FGO	1.2453	1.7897	2.4407	3.1324	3.8430
	FGX	1.1107	1.3909	1.7616	2.1769	2.6157
$\theta=30$	UD	1.1449	1.4976	1.9484	2.4437	2.9611
	FGV	1.1438	1.4943	1.9428	2.4356	2.9507
	FGO	1.2228	1.7266	2.3361	2.9873	3.6580
	FGX	1.1068	1.3783	1.7390	2.1444	2.5734
$\theta=45$	UD	1.1363	1.4714	1.9029	2.3790	2.8776
	FGV	1.1349	1.4669	1.8952	2.3680	2.8635
	FGO	1.1944	1.6450	2.1997	2.7972	3.4151
	FGX	1.1041	1.3698	1.7238	2.1225	2.5449
$\theta=60$	UD	1.1192	1.4180	1.8095	2.2458	2.7052
	FGV	1.1177	1.4130	1.8007	2.2331	2.6888
	FGO	1.1541	1.5256	1.9967	2.5119	3.0490
	FGX	1.0963	1.3445	1.6785	2.0569	2.4592
$\theta=75$	UD	1.0876	1.3160	1.6268	1.9816	2.3608
	FGV	1.0874	1.3152	1.6254	1.9797	2.3582
	FGO	1.1185	1.4158	1.8055	2.2400	2.6976
	FGX	1.0699	1.2563	1.5171	1.8203	2.1482

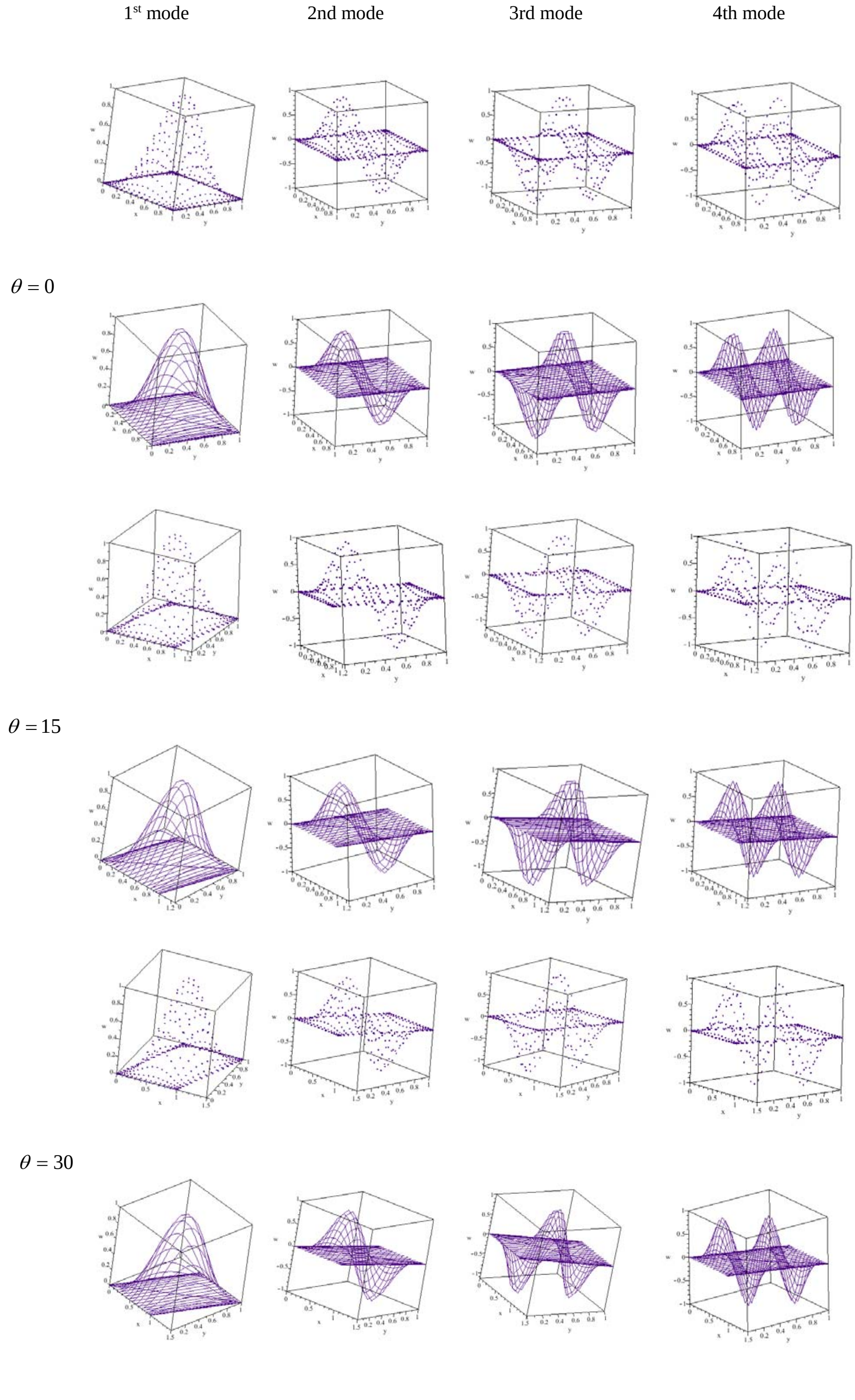
1st mode
2nd mode
3rd mode
4th mode
$\theta = 0$
$\theta = 15$
$\theta = 30$

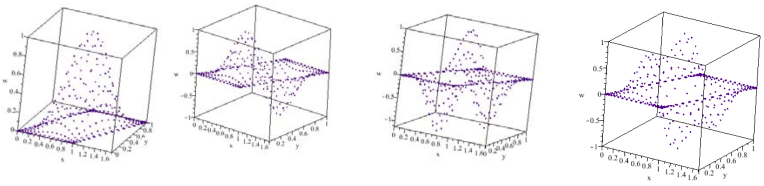

$\theta = 45$

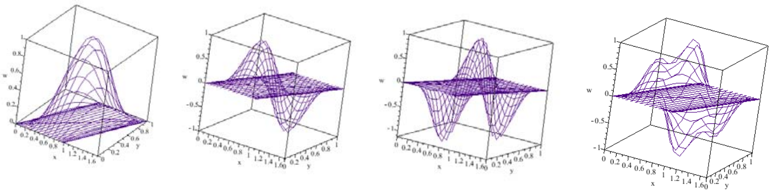

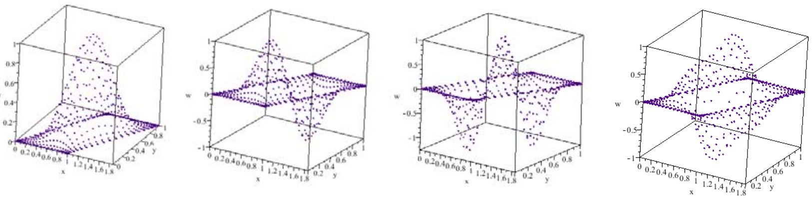

$\theta = 60$

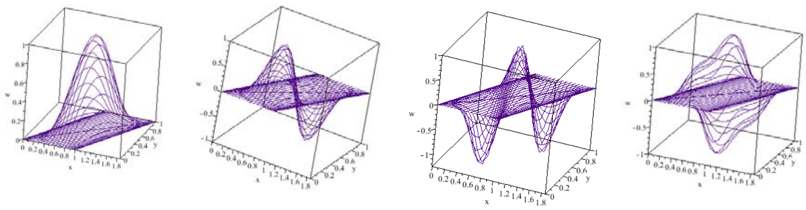

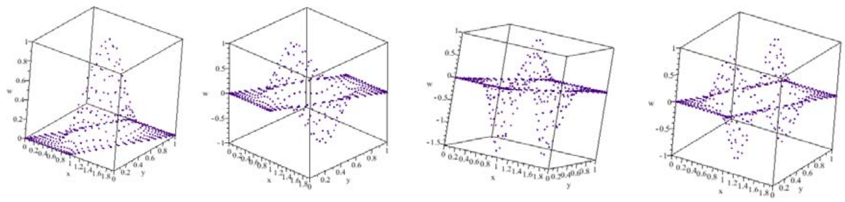

$\theta = 75$

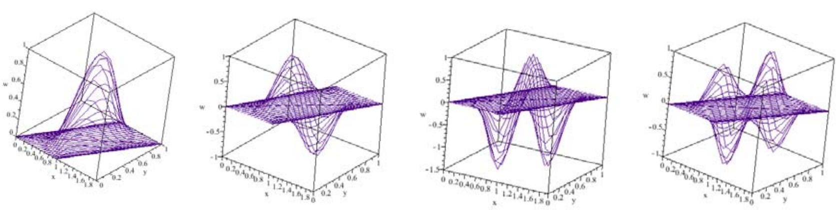

Figure 4: 3D vibration mode shapes of UD-CNTRC skew plate in fully clamped boundary conditions.

CNT on the nonlinear plate's vibration behavior are examined. Solving the problem leads to the following results.

1. The Differential quadrature method accompanying Frechet derivative Technique is an efficient method for solving the nonlinear couple differential equations.
2. For a skew plate reinforced with uniformly distributed carbon nanotubes, increase in skew angle of the plate result an increase in dimensionless frequency of the system.
3. In the reinforced skew plate with uniform distributions of carbon nanotubes, non-dimensional natural frequencies have been increased by increasing the volume fraction of carbon nanotubes.
4. In the linear analysis of FG-CNTRC skew plate in accordance with the FGO model, the non-dimensional natural frequencies are the minimum ones. UD, FGV, and FGX models result in higher frequencies. This happens for all kinds of boundary conditions.
5. Like other references in this study, it is concluded that for isotropic square plate and FG-CNTRC skew plate, the nonlinear frequency ratio increases with higher amplitudes of plate's vibration. This indicates hardening type of nonlinear behavior.
6. In nonlinear analysis of FG-CNTRC skew plate, the maximum nonlinear frequency ratio is related to the square plate. Its ratio decreases with the increased skew angle.
7. Nonlinear analysis of FG-CNTRC skew plate based on the FGO model results in the highest nonlinear frequency ratio. This ratio will be lower using UD, FGV and FGX models, respectively.
8. In case of $V_{cnt}=0.12$, the nonlinear frequency ratio would be maximum and by increasing the CNTs volume fraction the nonlinear frequency ratio decreases.
9. The degree of hardening type of non-linearity is less for clamped boundary condition compared to those of simply supported boundary condition.

Appendix: Equations of force, moment and stress resultants in terms of displacement

$$\begin{aligned}N_x=&A_{11}\left(\frac{\partial u}{\partial x}+\frac{1}{2}\left(\frac{\partial u}{\partial x}\right)^2+\frac{1}{2}\left(\frac{\partial v}{\partial x}\right)^2+\frac{1}{2}\left(\frac{\partial w}{\partial x}\right)^2\right)+B_{11}\left(-\frac{\partial^2 w}{\partial x^2}-\frac{\partial u}{\partial x}\frac{\partial^2 w}{\partial x^2}-\frac{\partial v}{\partial x}\frac{\partial^2 w}{\partial x\partial y}\right)\\&+D_{11}\left(\frac{1}{2}\left(\frac{\partial^2 w}{\partial x^2}\right)^2+\frac{1}{2}\left(\frac{\partial^2 w}{\partial x\partial y}\right)^2\right)+A_{12}\left(\frac{\partial v}{\partial y}+\frac{1}{2}\left(\frac{\partial u}{\partial y}\right)^2+\frac{1}{2}\left(\frac{\partial v}{\partial y}\right)^2+\frac{1}{2}\left(\frac{\partial w}{\partial y}\right)^2\right)\\&+B_{12}\left(-\frac{\partial^2 w}{\partial y^2}-\frac{\partial v}{\partial y}\frac{\partial^2 w}{\partial y^2}-\frac{\partial u}{\partial y}\frac{\partial^2 w}{\partial x\partial y}\right)+D_{12}\left(\frac{1}{2}\left(\frac{\partial^2 w}{\partial y^2}\right)^2+\frac{1}{2}\left(\frac{\partial^2 w}{\partial x\partial y}\right)^2\right),\end{aligned}\tag{A.1}$$

$$
\begin{aligned}
N_y = & A_{12}\left(\frac{\partial u}{\partial x}+\frac{1}{2}\left(\frac{\partial u}{\partial x}\right)^2+\frac{1}{2}\left(\frac{\partial v}{\partial x}\right)^2+\frac{1}{2}\left(\frac{\partial w}{\partial x}\right)^2\right)+B_{12}\left(-\frac{\partial^2 w}{\partial x^2}-\frac{\partial u}{\partial x}\frac{\partial^2 w}{\partial x^2}-\frac{\partial v}{\partial x}\frac{\partial^2 w}{\partial x\partial y}\right)\\
&+D_{12}\left(\frac{1}{2}\left(\frac{\partial^2 w}{\partial x^2}\right)^2+\frac{1}{2}\left(\frac{\partial^2 w}{\partial x\partial y}\right)^2\right)+A_{22}\left(\frac{\partial v}{\partial y}+\frac{1}{2}\left(\frac{\partial u}{\partial y}\right)^2+\frac{1}{2}\left(\frac{\partial v}{\partial y}\right)^2+\frac{1}{2}\left(\frac{\partial w}{\partial y}\right)^2\right)\\
&+B_{22}\left(-\frac{\partial^2 w}{\partial y^2}-\frac{\partial v}{\partial y}\frac{\partial^2 w}{\partial y^2}-\frac{\partial u}{\partial y}\frac{\partial^2 w}{\partial x\partial y}\right)+D_{22}\left(\frac{1}{2}\left(\frac{\partial^2 w}{\partial y^2}\right)^2+\frac{1}{2}\left(\frac{\partial^2 w}{\partial x\partial y}\right)^2\right),
\end{aligned}
\tag{A.2}
$$

$$
\begin{aligned}
N_{xy} = & A_{66}\left(\frac{\partial u}{\partial y}+\frac{\partial v}{\partial x}+\frac{\partial u}{\partial x}\frac{\partial u}{\partial y}+\frac{\partial v}{\partial x}\frac{\partial v}{\partial y}+\frac{\partial w}{\partial x}\frac{\partial w}{\partial y}\right)\\
&+B_{66}\left(-2\frac{\partial^2 w}{\partial x\partial y}-\frac{\partial u}{\partial x}\frac{\partial^2 w}{\partial x\partial y}-\frac{\partial u}{\partial y}\frac{\partial^2 w}{\partial x^2}-\frac{\partial v}{\partial x}\frac{\partial^2 w}{\partial y^2}-\frac{\partial v}{\partial y}\frac{\partial^2 w}{\partial x\partial y}\right)\\
&+D_{66}\left(\frac{\partial^2 w}{\partial x^2}\frac{\partial^2 w}{\partial x\partial y}+\frac{\partial^2 w}{\partial y^2}\frac{\partial^2 w}{\partial x\partial y}\right),
\end{aligned}
\tag{A.3}
$$

$$
\begin{aligned}
M_x = & B_{11}\left(\frac{\partial u}{\partial x}+\frac{1}{2}\left(\frac{\partial u}{\partial x}\right)^2+\frac{1}{2}\left(\frac{\partial v}{\partial x}\right)^2+\frac{1}{2}\left(\frac{\partial w}{\partial x}\right)^2\right)+D_{11}\left(-\frac{\partial^2 w}{\partial x^2}-\frac{\partial u}{\partial x}\frac{\partial^2 w}{\partial x^2}-\frac{\partial v}{\partial x}\frac{\partial^2 w}{\partial x\partial y}\right)\\
&+F_{11}\left(\frac{1}{2}\left(\frac{\partial^2 w}{\partial x^2}\right)^2+\frac{1}{2}\left(\frac{\partial^2 w}{\partial x\partial y}\right)^2\right)+B_{12}\left(\frac{\partial v}{\partial y}+\frac{1}{2}\left(\frac{\partial u}{\partial y}\right)^2+\frac{1}{2}\left(\frac{\partial v}{\partial y}\right)^2+\frac{1}{2}\left(\frac{\partial w}{\partial y}\right)^2\right)\\
&+D_{12}\left(-\frac{\partial^2 w}{\partial y^2}-\frac{\partial v}{\partial y}\frac{\partial^2 w}{\partial y^2}-\frac{\partial u}{\partial y}\frac{\partial^2 w}{\partial x\partial y}\right)+F_{12}\left(\frac{1}{2}\left(\frac{\partial^2 w}{\partial y^2}\right)^2+\frac{1}{2}\left(\frac{\partial^2 w}{\partial x\partial y}\right)^2\right),
\end{aligned}
\tag{A.4}
$$

$$
\begin{aligned}
M_y = & B_{12}\left(\frac{\partial u}{\partial x}+\frac{1}{2}\left(\frac{\partial u}{\partial x}\right)^2+\frac{1}{2}\left(\frac{\partial v}{\partial x}\right)^2+\frac{1}{2}\left(\frac{\partial w}{\partial x}\right)^2\right)+D_{12}\left(-\frac{\partial^2 w}{\partial x^2}-\frac{\partial u}{\partial x}\frac{\partial^2 w}{\partial x^2}-\frac{\partial v}{\partial x}\frac{\partial^2 w}{\partial x\partial y}\right)\\
&+F_{12}\left(\frac{1}{2}\left(\frac{\partial^2 w}{\partial x^2}\right)^2+\frac{1}{2}\left(\frac{\partial^2 w}{\partial x\partial y}\right)^2\right)+B_{22}\left(\frac{\partial v}{\partial y}+\frac{1}{2}\left(\frac{\partial u}{\partial y}\right)^2+\frac{1}{2}\left(\frac{\partial v}{\partial y}\right)^2+\frac{1}{2}\left(\frac{\partial w}{\partial y}\right)^2\right)\\
&+D_{22}\left(-\frac{\partial^2 w}{\partial y^2}-\frac{\partial v}{\partial y}\frac{\partial^2 w}{\partial y^2}-\frac{\partial u}{\partial y}\frac{\partial^2 w}{\partial x\partial y}\right)+F_{22}\left(\frac{1}{2}\left(\frac{\partial^2 w}{\partial y^2}\right)^2+\frac{1}{2}\left(\frac{\partial^2 w}{\partial x\partial y}\right)^2\right),
\end{aligned}
\tag{A.5}
$$

$$
\begin{aligned}
M_{xy} = & B_{66}\left(\frac{\partial u}{\partial y}+\frac{\partial v}{\partial x}+\frac{\partial u}{\partial x}\frac{\partial u}{\partial y}+\frac{\partial v}{\partial x}\frac{\partial v}{\partial y}+\frac{\partial w}{\partial x}\frac{\partial w}{\partial y}\right)\\
&+D_{66}\left(-2\frac{\partial^2 w}{\partial x\partial y}-\frac{\partial u}{\partial x}\frac{\partial^2 w}{\partial x\partial y}-\frac{\partial u}{\partial y}\frac{\partial^2 w}{\partial x^2}-\frac{\partial v}{\partial x}\frac{\partial^2 w}{\partial y^2}-\frac{\partial v}{\partial y}\frac{\partial^2 w}{\partial x\partial y}\right)\\
&+F_{66}\left(\frac{\partial^2 w}{\partial x^2}\frac{\partial^2 w}{\partial x\partial y}+\frac{\partial^2 w}{\partial y^2}\frac{\partial^2 w}{\partial x\partial y}\right),
\end{aligned}
\tag{A.6}
$$

$$
\begin{aligned}
P_x = & D_{11}\left(\frac{\partial u}{\partial x}+\frac{1}{2}\left(\frac{\partial u}{\partial x}\right)^2+\frac{1}{2}\left(\frac{\partial v}{\partial x}\right)^2+\frac{1}{2}\left(\frac{\partial w}{\partial x}\right)^2\right)+F_{11}\left(-\frac{\partial^2 w}{\partial x^2}-\frac{\partial u}{\partial x}\frac{\partial^2 w}{\partial x^2}-\frac{\partial v}{\partial x}\frac{\partial^2 w}{\partial x\partial y}\right)\\
&+H_{11}\left(\frac{1}{2}\left(\frac{\partial^2 w}{\partial x^2}\right)^2+\frac{1}{2}\left(\frac{\partial^2 w}{\partial x\partial y}\right)^2\right)+D_{12}\left(\frac{\partial v}{\partial y}+\frac{1}{2}\left(\frac{\partial u}{\partial y}\right)^2+\frac{1}{2}\left(\frac{\partial v}{\partial y}\right)^2+\frac{1}{2}\left(\frac{\partial w}{\partial y}\right)^2\right)\\
&+F_{12}\left(-\frac{\partial^2 w}{\partial y^2}-\frac{\partial v}{\partial y}\frac{\partial^2 w}{\partial y^2}-\frac{\partial u}{\partial y}\frac{\partial^2 w}{\partial x\partial y}\right)+H_{12}\left(\frac{1}{2}\left(\frac{\partial^2 w}{\partial y^2}\right)^2+\frac{1}{2}\left(\frac{\partial^2 w}{\partial x\partial y}\right)^2\right),
\end{aligned}
\tag{A.7}
$$

$$
\begin{aligned}
P_y = & D_{12}\left(\frac{\partial u}{\partial x}+\frac{1}{2}\left(\frac{\partial u}{\partial x}\right)^2+\frac{1}{2}\left(\frac{\partial v}{\partial x}\right)^2+\frac{1}{2}\left(\frac{\partial w}{\partial x}\right)^2\right)+F_{12}\left(-\frac{\partial^2 w}{\partial x^2}-\frac{\partial u}{\partial x}\frac{\partial^2 w}{\partial x^2}-\frac{\partial v}{\partial x}\frac{\partial^2 w}{\partial x\partial y}\right) \\
& +H_{12}\left(\frac{1}{2}\left(\frac{\partial^2 w}{\partial x^2}\right)^2+\frac{1}{2}\left(\frac{\partial^2 w}{\partial x\partial y}\right)^2\right)+D_{22}\left(\frac{\partial v}{\partial y}+\frac{1}{2}\left(\frac{\partial u}{\partial y}\right)^2+\frac{1}{2}\left(\frac{\partial v}{\partial y}\right)^2+\frac{1}{2}\left(\frac{\partial w}{\partial y}\right)^2\right) \\
& +F_{22}\left(-\frac{\partial^2 w}{\partial y^2}-\frac{\partial v}{\partial y}\frac{\partial^2 w}{\partial y^2}-\frac{\partial u}{\partial y}\frac{\partial^2 w}{\partial x\partial y}\right)+H_{22}\left(\frac{1}{2}\left(\frac{\partial^2 w}{\partial y^2}\right)^2+\frac{1}{2}\left(\frac{\partial^2 w}{\partial x\partial y}\right)^2\right), \qquad \text{(A.8)}
\end{aligned}
$$

$$
\begin{aligned}
P_{xy} = & D_{66}\left(\frac{\partial u}{\partial y}+\frac{\partial v}{\partial x}+\frac{\partial u}{\partial x}\frac{\partial u}{\partial y}+\frac{\partial v}{\partial x}\frac{\partial v}{\partial y}+\frac{\partial w}{\partial x}\frac{\partial w}{\partial y}\right) \\
& +F_{66}\left(-2\frac{\partial^2 w}{\partial x\partial y}-\frac{\partial u}{\partial x}\frac{\partial^2 w}{\partial x\partial y}-\frac{\partial u}{\partial y}\frac{\partial^2 w}{\partial x^2}-\frac{\partial v}{\partial x}\frac{\partial^2 w}{\partial y^2}-\frac{\partial v}{\partial y}\frac{\partial^2 w}{\partial x\partial y}\right) \\
& +H_{66}\left(\frac{\partial^2 w}{\partial x^2}\frac{\partial^2 w}{\partial x\partial y}+\frac{\partial^2 w}{\partial y^2}\frac{\partial^2 w}{\partial x\partial y}\right). \qquad \text{(A.9)}
\end{aligned}
$$

Acknowledgements

This work was supported by Islamic Azad University of Arak branch, Arak Iran. Particularly, the author would like to express his sincere thanks for their inspiring communication.

References

[1] M. SINGHA AND R. DARIPA, *Nonlinear vibration of symmetrically laminated composite skew plates by finite element method*, Int. J. Nonlinear Mech., 42 (1996), pp. 1144–1152.

[2] P. MALEKZADEH, *A differential quadrature nonlinear free vibration analysis of laminated composite skew thin plates*, Thin-Walled Structures, 45 (2007), pp. 237–250.

[3] A. UPADHYAY AND K. SHUKLA, *Geometrically nonlinear static and dynamic analysis of functionally graded skew plates*, Commun. Nonlinear Sci. Numer. Simulation, 18 (2013), pp. 2252–2279.

[4] P. MALEKZADEH, *Differential quadrature large amplitude free vibration analysis of laminated skew plates based on FSDT*, Composite Structures, 83 (2008), pp. 189–200.

[5] Z. LEI, L. ZHANG AND K. LIEW, *Meshless modeling of geometrically nonlinear behavior of CNT-reinforced functionally graded composite laminated plates*, Appl. Math. Comput., 295 (2017), pp. 24–46.

[6] M. KELESHTERI, H. ASADI AND Q. WANG, *Large amplitude vibration of FG-CNT reinforced composite annular plates with integrated piezoelectric layers on elastic foundation*, Thin-Walled Structures, 120 (2017), pp. 203–214.

[7] P. MALEKZADEH AND A. ZAREI, *Free vibration of quadrilateral laminated plates with carbon nanotube reinforced composite layers*, Thin-Walled Structures, 82 (2014), pp. 221–232.

[8] L. ZHANG, Z. LEI AND K. LIEW, *Vibration characteristic of moderately thick functionally graded carbon nanotube reinforced composite skew plates*, Composite Structures, 122 (2015), pp. 172–183.

[9] P. MALEKZADEH AND M. DEHBOZORGI, *Low velocity impact analysis of functionally graded carbon nanotubes reinforced composite skew plates*, Composite Structures, 140 (2016), pp. 728–748.

[10] Y. KIANI, *Free vibration of FG-CNT reinforced composite skew plates*, Aerospace Sci. Tech., 58 (2016), pp. 178–188.

[11] L. ZHANG AND L. XIAO, *Mechanical Behavior of laminated CNT-reinforced composite skew plates subjected to dynamic loading*, Composite Part B, 122 (2017), pp. 219–230.

[12] ENRIQUE GARCÍA, RAFAEL CASTRO AND ERICK I. SAAVEDRA FLORES, *Static and free vibration analysis of functionally graded carbon nanotube reinforced skew plates*, Composite Structures.

[13] L. W. ZHANG, Z. X. LEI AND K. M. LIEW, *Vibration characteristic of moderately thick functionally graded carbon nanotube reinforced composite skew plates*, Composite Structures, (2014).

[14] Y. S. SHIH AND P. T. BLOTTER, *Nonlinear vibration analysis of arbitrarily laminated thin rectangular plates on elastic foundations,* J. Sound Vib., 167 (1993), pp. 433–459.

[15] M. K. SINGHA AND RUPESH DARIPA, *Nonlinear vibration of symmetrically laminated composite skewplates byfinite element method*, Int. J. Nonlinear Mech., 42 (2007), pp. 1144–1152.

[16] C. W. BERT AND M. MALIK, *Differential quadrature method in computational mechanics*, areview, Appl. Mech. Rev., 49 (1996), pp. 1–27.

[17] S. L. LAU, Y. K. CHEUNG AND S. Y. WU, *Nonlinear vibration of thin-elastic plates, Part 1: Generalized incremental Hamilton's principle and element formulation,* ASME J. Appl. Mech., 51 (1984), pp. 837–844.

[18] MALOY K. SINGHA AND M. GANAPATHI, *Large amplitude free flexural vibrations of laminated composite skew plates*, Int. J. Nonlinear Mech., 39 (2004), pp. 1709–1720.

[19] H. N. CHU AND G. HERRMANN, *Influence of large amplitudes on free flexural vibrations of rectangular plates,* ASME, J. Appl. Mech., 23 (1956), pp. 532–540.

[20] S. R. RAO, A. H. SHEIKH AND M. MUKHOPADHYAY, *Large amplitude finite element flexural vibration of plates/stiffened plate,* J. Acoust. Society Am., 93 (1993), pp. 3250–3257.